The International Journal of Biochemistry & Cell Biology 45 (2013) 1720–1729

Contents lists available at SciVerse ScienceDirect

The International Journal of Biochemistry & Cell Biology

journal homepage: www.elsevier.com/locate/biocel

Identification of DAPK as a scaffold protein for the LIMK/cofilin complex in TNF-induced apoptosis

Jelena Ivanovska[a], Alexandra Tregubova[a], Vijayalakshmi Mahadevan[b], Saritha Chakilam[a], Muktheshwar Gandesiri[a], Natalya Benderska[a], Benjamin Ettle[a], Arndt Hartmann[a], Stephan Söder[a], Elisabeth Ziesché[c], Thomas Fischer[d], Lena Lautscham[e], Ben Fabry[e], Gabriela Segerer[f], Antje Gohla[f], Regine Schneider-Stock[a,*]

[a] Experimental Tumorpathology, Department of Pathology, University of Erlangen-Nuremberg, Germany
[b] Faculty of School of Chemical & Biotechnology of the SASTRA University, Thanjavur, India
[c] 3rd Medical Department, Medical University, Mainz, Germany
[d] Center of Internal Medicine, Department of Hematology/Oncology, Otto-von-Guericke University Magdeburg, Germany
[e] Department of Physics, University of Erlangen-Nuremberg, Germany
[f] Institute for Pharmacology and Rudolf Virchow Center for Experimental Biomedicine, University of Würzburg, Germany

ARTICLE INFO

Article history:
Received 21 November 2012
Received in revised form 9 April 2013
Accepted 9 May 2013
Available online xxx

Keywords:
TNF
DAPK
LIMK
Cofilin
Apoptosis

ABSTRACT

The role of cytoskeleton-associated proteins during TNF-induced apoptosis is not fully understood. A potential candidate kinase that might connect TNF signaling to actin reorganization is the death-associated protein kinase (DAPK). To identify new DAPK interaction partners in TNF-induced apoptosis, we performed a peptide array screen. We show that TNF-treatment enhanced the phosphorylation of LIMK at threonine508 and its downstream target cofilin at serine3 (p-cofilin^{Ser3}). Modulation of DAPK activity and expression by DAPK inhibitor treatment, siRNA knockdown, and overexpression affected the phosphorylation of both proteins. We propose a 3D structural model where DAPK functions as a scaffold for the LIMK/cofilin complex and triggers a closer interaction of both proteins under TNF stimulation. Upon TNF a striking redistribution of LIMK, DAPK, and cofilin to the perinuclear compartment was observed. The pro-apoptotic DAPK/LIMK/cofilin multiprotein complex was abrogated in detached cells, indicating that its signaling was no longer needed if cells committed to apoptosis. P-cofilin^{Ser3} was strongly accumulated in cells with condensed chromatin, pronounced membrane blebs and Annexin V up-regulation. From studying different cofilin^{Ser3} mutants we suggest that p-cofilin^{Ser3} is an indicator of TNF-induced apoptosis. Collectively, our findings identify a novel molecular cytoskeleton-associated mechanism in TNF-induced DAPK-dependent apoptosis.

1. Introduction

Tumor necrosis factor (TNF) is a pro-inflammatory mediator with the capacity to induce apoptosis (Benderska et al., 2012). Recent reports have shown that TNF might trigger cell death, at least in part, by directly affecting the reorganization of the actin cytoskeleton (Campos et al., 2009). The most apparent consequences of TNF-induced apoptosis are drastic changes in cell morphology – such as the rounding-up of the cell and blebbing of the plasma membrane (Mathew et al., 2009; Scanlon et al., 1989). Nevertheless, the responsible cytoskeletal proteins and their signaling pathways are not well understood.

A potential candidate kinase that might connect TNF signaling to actin reorganization during cell death is the death-associated protein kinase (DAPK), a calmodulin-regulated and actin filament-associated serine/threonine kinase (Deiss et al., 1995). DAPK is known to exert tumor-suppressive functions, and this has been attributed to its apoptosis-promoting activity (Deiss et al., 1995; Inbal et al., 1997, 2000; Kögel et al., 2003; Raveh and Kimchi, 2001). DAPK exerts this pro-apoptotic effect by inside-out inactivation of integrin β1, thereby suppressing the matrix survival signal and activating a p53-dependent apoptosis pathway (Wang et al., 2002). It also participates in TNF- and Fas-induced apoptosis (Cohen et al., 1997). However, despite of a broad involvement in different cell death systems, very little is known about DAPK's role in cytoskeletal reorganization.

DAPK's localization to specific cytoskeletal components might bring it into close proximity with its physiological substrates. One known cytoskeletal-associated substrate of DAPK is the myosin-II

* Corresponding author at: Institute for Pathology Universitätsstraße 22, 91054 Erlangen, Germany. Tel.: +49 9131 85 26070; fax: +49 9131 85 26197.
E-mail address: regine.schneider-stock@uk-erlangen.de (R. Schneider-Stock).

1357-2725/$ – see front matter © 2013 Elsevier Ltd. All rights reserved.
http://dx.doi.org/10.1016/j.biocel.2013.05.013

light chain (MLC), which has previously been shown to be phosphorylated by DAPK, thus stabilizing actin stress fibers (Cohen et al., 1997; Kuo et al., 2003). Moreover, paxillin, a component of focal adhesions, was found to be localized in close proximity to the tips of the DAPK-positive filaments, indicating that stress fibers containing DAPK extend to focal contacts (Bialik and Kimchi, 2004, 2006). Recently we have shown that activation of the p38/DAPK complex induces caspase3-dependent apoptotic cell death under TNF stimulation (Bajbouj et al., 2009). The signaling molecules involved in the TNF-mediated downstream pathway between DAPK and caspase3 have not yet been identified. We performed a phospho-peptide array to test for cytoskeleton-associated proteins that might interact with DAPK under TNF stimulation. We found that cofilin1 showed a marked increase in phosphorylation at serine3 residue in response to TNF. Cofilin1 is a key regulator of actin filament dynamics and reorganization by stimulating depolymerisation and severing of actin filaments (Bamburg et al., 1999; Bernstein and Bamburg, 2010; Moon and Drubin, 1995; Pollard and Borisy, 2003). The activity of cofilin is reversibly regulated by phosphorylation and dephosphorylation at serine3, with the phosphorylated form being inactive. LIM kinase1 (LIMK1) phosphorylates cofilin and thereby inhibits its actin filament-disrupting activity (Arber et al., 1998; Yang et al., 1998). The inactive serine3-phosphorylated cofilin (p-cofilin^{Ser3}) is dephosphorylated and reactivated by phosphatases of the Slingshot family and by Chronophin (Gohla et al., 2005; Niwa et al., 2002). LIMK1-mediated cofilin phosphorylation is critically involved in a variety of physiological and pathological processes, including directional migration, chemotaxis, cell polarity and tumor invasion (Aizawa et al., 2001; Kobayashi et al., 2006; Mouneimne et al., 2006; Nishita et al., 2005; Yoshioka et al., 2003). Its role in apoptosis, however, is not well investigated.

Using a biochemical and cell biological approach we identified a DAPK1/LIMK1/cofilin1 pro-apoptotic multi-protein complex. We suggest that DAPK acts as a scaffold protein for the LIMK/cofilin complex under TNF stimulation. Our findings elucidate a molecular mechanism that connects TNF-induced DAPK activation to the profound actin cytoskeletal rearrangements typical of apoptotic cells.

2. Materials and methods

2.1. Cell culture and reagents

Human colon tumor cell line HCT116 (ATCC, Manassas, VA) was maintained in RPMI with 10% fetal bovine serum, penicillin (100 U/ml), and streptomycin (100 μg/ml). Cells were incubated at 37 °C in a humidified atmosphere of 5% CO_2. Cells were stimulated with 0.66 ng/ml TNF (Immunotools) in RPMI medium for 1, 6, 24, 48 and 72 h, as described previously (Bajbouj et al., 2009). The unstimulated cells cultured for 24 h were considered as the control. DAPK1 inhibitor (4Z)-2-phenyl-4-(pyridin-3-ylmethylidene)-4,5-dihydro-1,3-oxazol-5-one (MolPort). Cells were pre-treated for 60 min with 25 μM DAPK inhibitor.

2.2. Western blotting

The protein concentrations were measured with Bio-Rad DC protein Assay (BioRad Laboratories). Equal protein content (30 μg) of cell lysates were separated on denaturing SDS-PAGE and transferred onto nitrocellulose membrane and then probed with antibodies as indicated. Antibodies used were: Anti-DAPK (BD Transduction Laboratories), anti-phospho DAPK^{Ser308} (Sigma), anti-LIMK1, anti-phospho LIMK1^{Thr508}, anti-cofilin1 (Santa Cruz Biotechnology), anti-phospho cofilin1^{Ser3}, anti-caspase3, anti-caspase8, anti-caspase9 (Cell signaling), and with secondary antibodies (anti-mouse, anti-goat or anti-rabbit IgG peroxidise conjugated; Pierce). Bound antibodies were visualized using West Pico chemiluminescent substrate (Pierce) according to the manufacturer's instructions. Immunobloting with anti-GAPDH was used to control equal loading and protein quality. Images were performed using GeneGnome (Syngene). Image J analysis software (version 1.45s) was used to quantify band intensities.

2.3. Immunoprecipitation

HCT116 cells were lysed in RIPA lysis buffer (50 mmol/l Tris–HCl pH 8150 mmol/l NaCl, 1%NP40) containing 1 mmol/l phenylmethylsulfonyl fluoride and 1:100 of Protease Inhibitor Cocktail Set III (Calbiochem) at 4 °C for 15 min and were sonicated. Cell debris was removed after centrifugation and protein contents were estimated using the Bradford method. For immunoprecipitation, lysates were incubated with magnetic beads Protein G Dynabeads (Invitrogen) according to manufacturer's instructions and with anti-DAPK, anti-LIMK1 and anti-cofilin1 antibodies. Protein G Dynabeads incubated with antibody without lysate were considered as IgG control. Protein separation was performed by SDS-PAGE gel electrophoresis, followed by Western blotting procedure.

2.4. Plasmids, transfections, mutagenesis and si RNA

Full length LIMK construct was in pcDNA-3 and human cofilin 1 was cloned in pCMV6 – His6 (C-terminal) via Kpn I and Cla I (Promega, Madison, WI, USA), pRK5F–DAPK expression vector was a gift from Dr. Ruey-Hwa Chen (Institute of Molecular Medicine, National Taiwan University Hospital, Taipei, Taiwan). Transient transfection was performed using Invitrogen's lipofectamin 2000 according to the manufacturer's recommendations. Briefly, HCT wt cells were grown in six-well plates and transfected using 0.5–2 μg of plasmid cDNA. Medium was changed 4–6 h after transfection. Transfected cells were grown in the presence or absence of 0.66 ng/ml TNF for 6 and 24 h. Appropriate empty vector without TNF-treatment was used as a transfection negative control. Site-directed mutagenesis was performed by PCR on plasmid DNA for cofilin1 construct and verified by sequencing. Cofilin1^{Ser3} mutants were obtained by substitutions of the indicated amino acid residue by alanine, glutamic and aspartic acid. Primers containing phosphate group on the 5′end were used: Ala3 5′-Pho-**GCC**GGTGTGGCTGTCTCTGATGGT-GTCATCAAGGT-3′; Glu3 5′-Pho-**GAG**GGTG TGGCTGTCTCTGATGGTGTCATCAAGGT-GTT-3′; Asp3 5′-Pho-**GAC**GGTGTGGCTGTCTCTGATGGTGTCATCAAGGTGTT-3′ (Metabion). All siRNA reagents were obtained from Thermo Fisher Scientific (Dharmacon RNAi Technologies). DAPK- or LIMK-specific siRNA were used at final concentration of 25–100 nM. DharmaFECT transfection reagent was used for 24 h for transfection of siRNA on sub-confluent cells, according to manufacturer's instructions.

2.5. Annexin V/Propidium Iodide (PI) staining

Apoptosis was assessed used Annexin-V-FLUOS kit (Roche Diagnostic GmbH). Cells were transfected as described above for 24 h and stimulated with 0.66 ng/ml TNF for 24 h. At the end of the incubation period, floating as well as adherent cells were harvested by trypsinisation and washed twice with PBS. 1×10^6 cells were stained with 100 μl annexin V/PI solution (20 μl FITC-conjugated annexin V reagent (20 μg/ml) + 20 μl PI reagent (50 μg/ml in 1 ml of dilution/HEPES buffer) for 15 min at RT in dark. Cell suspension was diluted by adding appropriate amount of dilution buffer and analyzed using FACS Calibur flow cytometer (BD).

2.6. Immunofluorescence analysis and microscopic observation

HCT116 cells grown on glass coverslips were either treated with TNF for 24 and 48 h or untreated, and then fixed in 3% paraformaldehyde for 15 min followed by incubation with 0.2% Triton X-100 for 5 min at room temperature and washed with PBS. Fixed cells were incubated with blocking buffer 1% BSA in PBS and then immunofluorescence staining was performed with anti-phospho cofilin1^{Ser3} (1:500), anti-cofilin (1:500), anti-phospho-LIMK^{Thr508} (1:500), anti-LIMK (1:500) and anti-DAPK (1:250). To detect apoptosis the FITC-conjugated annexin V reagent from Annexin-V-FLUOS kit (Roche Diagnostics) was used. Appropriate Alexa Fluor 488-, 647-or 555-conjugated secondary antibodies (Invitrogen) were used at 1:500. Cells were mounted on slides with ProLong Gold antifade reagent with DAPI (Invitrogen) according to manufacturer's instructions. Immunofluorescence images were acquired on an inverted microscope Nikon eclipse T*i*-U (Tokyo, Japan) using 40× air and 100× oil objective lens (Nikon). Confocal images for cofilin, p-cofilin^{Ser3}, LIMK, pLIMK^{Thr508} and DAPK staining were obtained on a Confocal Laser Scanning Microscopy system (LSM T-PMT Observer Z1, Carl Zeiss Inc.), with a 63× oil objective.

2.7. Structural analysis of DAPK1–LIMK1–cofilin1 complex

To understand the interactions between cofilin1 and LIMK1, the structures of these proteins deposited in the PDB (cofilin: 1Q8G- NMR structure of human cofilin; LIMK1: 3S95- Xray structure of the kinase domain (residue 330–637) of human LIMK1 at 1.65 Å resolution) were considered (Beltrami et al., 2013; Pope et al., 2004). The docking, energy filtering and ranking of the complexes of these two structures were done by the ClusPro server (http://nrc.bu.edu/cluster) (Kozakov et al., 2010). The catalytic domain of DAPK1 (PDB: 1JKS – X-ray structure of the catalytic domain of human DAPK at 1.5 Å resolution) was then docked to the complex of cofilin and LIMK1 and ranking was done using ClusPro server (Tereshko et al., 2001). In both cases, the top 1000 structures were chosen after energy filtering (electrostatics), clustered and ranked according to cluster sizes. The cluster scores of the complexes from the ClusPro server were used to understand the energy profiles of the LIMK1–cofilin complex and that of the DAPK–LIMK1–cofilin complex. The hydrogen bond interactions in the LIMK1–cofilin complex were analyzed using HBOND Calculator (http://cib.cf.ocha.ac.jp/bitool/HBOND/) and are summarized in Table 1a. All renderings were performed using CHIMERA (Petsko and Ringe, 2004).

2.8. Peptide array

HCT116 human colorectal tumor cells were cultured for 6–72 h in either normal or TNF-conditioned medium. Kinase substrates (11 amino acid peptides) dotted as triplicates on a *PepChip kinase full slide* array (Pepscan) were radioactively labeled by incubation with cellular lysates supplemented with γ-33P-ATP for 2 h at 37 °C according to the manufacturer's instructions (Pepscan). This allowed kinase profiling by screening of 1024 substrates in triplicates.

2.9. Analysis of fluorescence intensities

Hoechst 33342 and p-cofilin^{Ser3} stained fluorescent images were background corrected and normalized to the maximum intensity. Hoechst images were binarized, and the average fluorescence intensity and the center position of each nucleus were computed. The average p-cofilin^{Ser3} fluorescence intensity of each cell was measured within a radius of 3 μm around the center of the detected nuclei.

2.10. Statistical analysis

Statistical analyses were accomplished using ANOVA test performed with software programme SPSS (SPSS Inc.). Statistical significance was defined as $P \leq 0.05$.

3. Results

3.1. LIMK/p-cofilin^{Ser3} pathway is activated in TNF-treated HCT116 cells

Recently, we have identified a pro-apoptotic role of the cytoskeleton-associated protein DAPK in TNF-induced apoptosis (Bajbouj et al., 2009). In order to identify new potential interaction partners of DAPK after TNF-treatment, we performed a phospho-peptide array. This array revealed more than 100 phosphorylated, up-regulated proteins upon treatment of HCT116 cells with TNF. We subsequently focused on proteins involved in cytoskeletal remodeling (Fig. S1A). An interesting candidate was cofilin, which was markedly phosphorylated on serine3 (p-cofilin^{Ser3}) after 48 h of TNF-treatment (Fig. S1B). A serine/threonine protein kinase directly upstream of cofilin is LIMK. To determine whether the response of human HCT116 colorectal tumor cells to TNF is associated with phosphorylation of LIMK1 (p-LIMK^{Thr508}) and cofilin, whole cell lysates of HCT116 cells stimulated with TNF were examined by Western blotting. TNF exposure induced phosphorylation of p-LIMK^{Thr508} within 6 h after TNF-treatment and a maximum of approximately

Table 1
(a) and (b) Analysis of interactions in the cofilin–LIMK docked complex and the cofilin–LIMK–DAPK docked complex.

(a) Cofilin–LIMK complex

Residue in cofilin	Residue in LIMK
Alanine 2	Tyrosine 507
Lysine 112	Serine 453
Glutamine 107	Lysine 386

(b) Cofilin–LIMK–DAPK complex

Residues in cofilin	Residues in LIMK	Residues in DAPK
Alanine 2	Tyrosine 507	
Lysine 112	Serine 453	
Lysine 112	Asparagine 455	
Glutamine 107	Lysine 386	
	Aspartate 568	Arginine 47
	Arginine 569	Lysine 50
	Proline 573	Phenylalanine 174
	Asparagine 574	Asparagine 172
	Glutamate 601	Lysine 50
	Histidine 602	Lysine 50
	Arginine 626	Glutamate 192
	Arginine 633	Valine 189

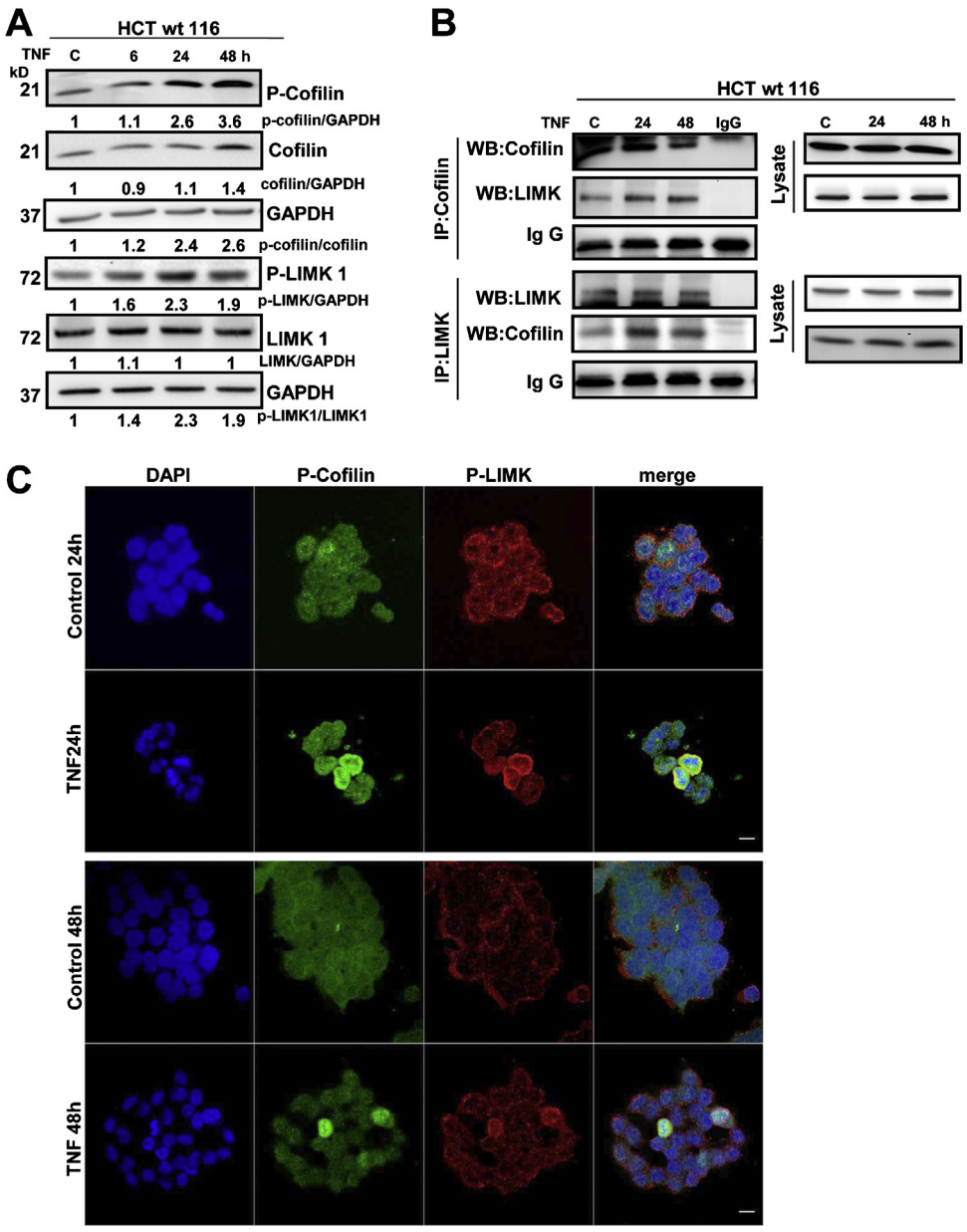

Fig. 1. Phosphorylation of LIMK^{Thr508} and cofilin^{Ser3} is up-regulated after TNF-stimulation in HCT116 cells. (A) Changes of p-LIMK^{Thr508} and p-cofilin^{Ser3} levels in cell lysates after 6, 24 and 48 h TNF-stimulation (0.66 ng/ml) was analyzed by Western blotting. Untreated HCT116 (c) served as a control. Results are representative of three independent experiments. The band intensities were quantified by densitometry analysis; the control was adjusted to one. (B) Cell lysates stimulated with TNF were immunoprecipitated (IP) and immunoblotted with anti-cofilin and anti-LIMK. The input cell lysates subjected to TNF, untreated HCT116 control cells (c) and IgG-IP served as a control. The data are representative of three independent experiments. (C) Distribution and co-localization of p-cofilin^{Ser3} and p-LIMK^{Thr508} after the TNF-treatment. Confocal immunofluorescence image of endogenous p-cofilin^{Ser3} (green), p-LIMK^{Thr508} (red) and DAPI (blue) staining in fixed HCT116 cells treated with TNF (0.66 ng/ml). The same confocal microscopy setup was used for all representative images. Bar 10 μm.

2.3-fold increase after 24 h in comparison to control (Fig. 1A). Furthermore, the level of p-cofilin^{Ser3} was positively correlated with the increase in p-LIMK^{Thr508} levels, starting from 6 h of TNF-stimulation and reaching a maximum increase of 2.6-fold over untreated control cell levels at 48 h (Fig. 1A). To verify that LIMK phosphorylated cofilin at serine3 in a TNF-dependent manner, we tested first by co-immunoprecipitation whether an intracellular complex was formed between LIMK and cofilin in HCT116 cells. Although a LIMK/cofilin complex was already detectable in untreated controls, it was strongly reinforced after TNF treatment for 24 and 48 h (Fig. 1B). Phosphorylation of LIMK and cofilin after TNF stimulation seems to occur with considerable time-delay. The LIMK/cofilin complex is already reinforced 24 h after TNF-stimulus indicating the possible starting time of cofilin phosphorylation and leading to cofilin phosphorylation and inactivation at later time point (48 h after TNF-treatment). Thus, there might be a delay in the initiation of the cofilin phosphorylation by LIMK. Furthermore, immunofluorescence confocal microscopy confirmed that p-cofilin^{Ser3} co-localized with p-LIMK^{Thr508} in the TNF-treated apoptotic cells with condensed chromatin (Fig. 1C). After LIMK siRNA mediated knockdown a remarkable down-regulation of LIMK was revealed. Nevertheless, the p-cofilin^{Ser3} level was not completely abolished (Fig. S2A). There are two possible explanations: one is the variable time frame where LIMK/cofilin phosphorylation occurs (24–48 h), another one is the possible contribution of cofilin regulatory phosphatases such as slingshot and chronophin (Gohla et al., 2005; Niwa et al., 2002). In the LIMK-overexpressing HCT116 cells the phosphorylation level of p-cofilin^{Ser3} was 2.3-fold higher (Fig. S2B) after 24 h of TNF-stimulation in comparison to transfected non-stimulated cells. Treatment of the cells with a 100-fold higher TNF concentration did not further elevate cofilin phosphorylation. These data indicate that LIMK interacts with cofilin, and that TNF-stimulation increases LIMK and cofilin phosphorylation in HCT116 tumor cells.

3.2. DAPK interferes with the TNF-induced LIMK/cofilin pathway

In order to investigate a potential link between the DAPK and LIMK/cofilin pathway, we analyzed if DAPK is a possible interaction partner of both proteins. Indeed, we found that DAPK co-precipitated with LIMK and cofilin in TNF-treated cells

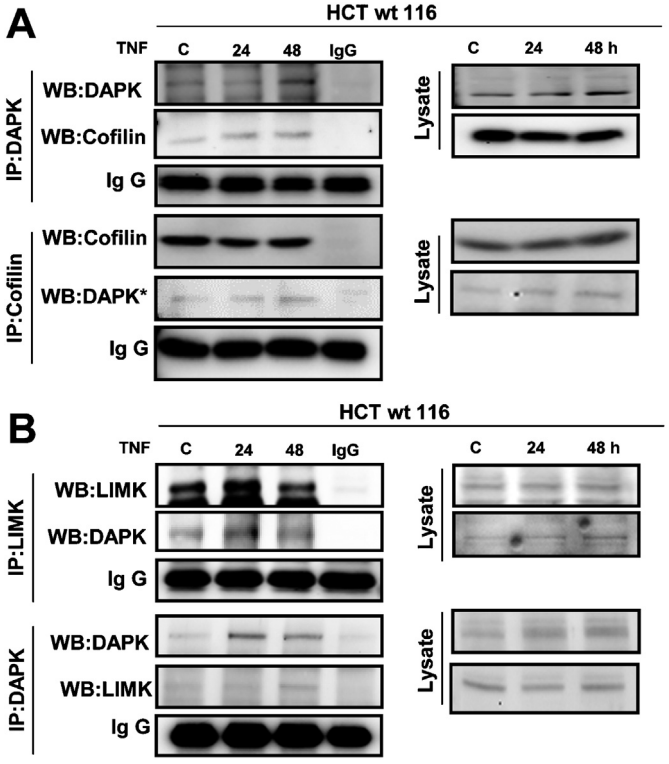

Fig. 2. TNF-induced complex formation between DAPK, LIMK and cofilin. Lysates obtained from TNF-stimulated cells were immunoprecipitated (IP) and immunoblotted with anti-cofilin (A), anti-DAPK (A and B) and anti-LIMK (B). The input cell lysates subjected to TNF, untreated HCT116 (c) and IgG-IP served as a control. The data are representative of three independent experiments. *Stronger signal at the left edge of the control DAPK band is transmitted from the signal of the protein marker.

(Fig. 2A and B), whereby the amount of DAPK in the complex was increased under TNF.

Next, we examined how the modulation of DAPK activity and DAPK expression affects the phosphorylation of LIMK and cofilin. First, we assessed the effects of DAPK inhibitory compound (4Z)-2-phenyl-4-(pyridin-3-ylmethylidene)-4,5-dihydro-1,3-oxazol-5-one (Okamoto et al., 2010; here referred to as "DAPK inhibitor") which we have recently shown to specifically inhibit the catalytic activity of DAPK (Gandesiri et al., 2012). One important aspect of DAPK functionality is that its kinase activity is decreased by autophosphorylation on serine308 (p-DAPK^{Ser308}) (Bialik and Kimchi, 2006). Hence, DAPK inhibition increased the levels of inactive DAPK (p-DAPK^{Ser308}) by 150% at 24 h, and by 350% at 48 h after TNF treatment (Fig. 3A) compared to TNF-treated cells without inhibitor (set at 100%). Importantly, the inhibition of DAPK activity revealed also decreased levels of p-LIMK^{Thr508} (42% reduction at 24 h, and 22% reduction at 48 h) and p-cofilin^{Ser3} (52% reduction at 48 h) compared to TNF-treated cells with unperturbed DAPK activity (set as 100%) (Fig. 3A).

We have previously shown that siRNA-mediated DAPK depletion attenuates TNF-induced apoptosis (Bajbouj et al., 2009); therefore we tested the influence of DAPK siRNA on LIMK/cofilin signaling. Although DAPK was present in the scrambled-si RNA treated cells we did not observe the expected increase in cofilin and LIMK phosphorylation after TNF treatment. This result might be due to the common problem in phosphorylation studies based on lipofectamin siRNAs that are known to interfere with receptor-mediated phosphorylation signaling suggesting that these cells have an attenuated response to TNF. However DAPK si knockdown in HCT116 cells reduced p-LIMK^{Thr508} levels after 24 h, and cofilin^{Ser3} phosphorylation after 48 h upon TNF-treatment compared to scrambled si RNA (Fig. 3B). Together these results suggest that lipofectamin transfected cells indeed showed a reduced response to TNF. We suggest that the decrease in cofilin and LIMK phosphorylation is a DAPK-dependent effect consistent with the findings from the DAPK inhibitor experiment. Because DAPK siRNA and DAPK inhibition reduced both LIMK^{Thr508} and cofilin^{Ser3} phosphorylation, we determined whether overexpressing DAPK would increase LIMK^{Thr508} and cofilin^{Ser3} phosphorylation (Fig. 3C). Indeed, TNF-treatment induced a 2.3-fold increase in p-cofilin^{Ser3} levels in the DAPK overexpressing cells. Cells with DAPK overexpression could not be analyzed at a later time point because transfection was highly cytotoxic to cells at 48 h after TNF treatment. We did not observe changes in LIMK^{Thr508} phosphorylation under our regular assay condition using 0.66 ng/ml TNF. Moreover, the levels of p-LIMK^{Thr508} were also only mildly elevated (by ~1.7-fold) with a 100-fold higher concentration of TNF (Fig. 3C). One explanation could be that DAPK overexpression inhibits the activity of cofilin phosphatases thereby stabilizing the p-cofilin^{Ser3}.

To better understand the role of DAPK in this multiprotein complex, we developed a 3D structural model of the possible interactions between cofilin, LIMK1, and DAPK. We docked cofilin and LIMK as a first step using the ClusPro server (Beltrami et al., 2013; Pope et al., 2004) (Fig. 4A, a and c). A thorough scan of the hydrogen

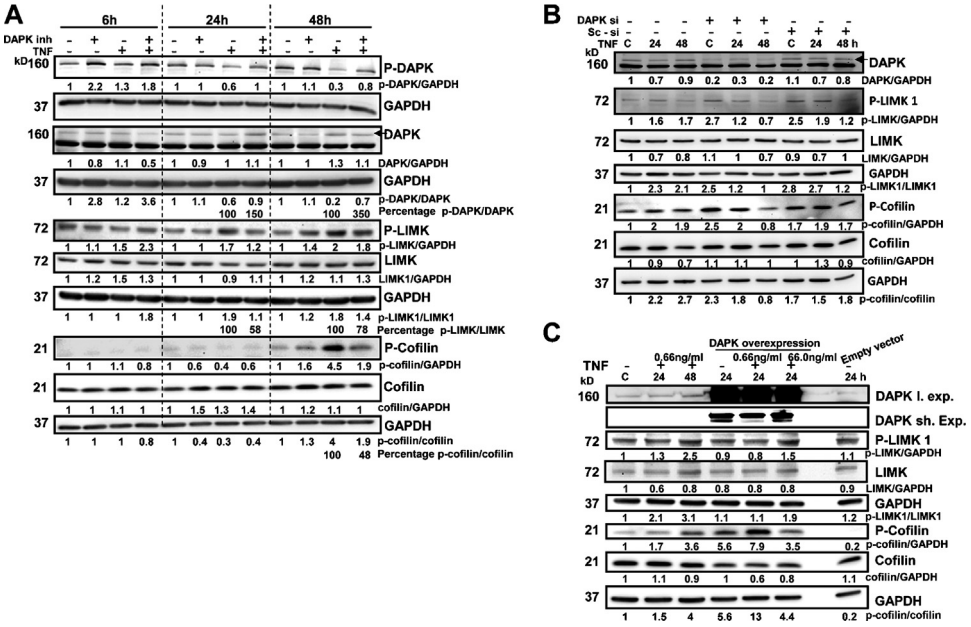

Fig. 3. DAPK is promoting LIMK/cofilin pathway under TNF-stimulation. (A) HCT116 cells were exposed to DAPK inhibitor 1 h before TNF-treatment (0.66 ng/ml) for 6, 24 and 48 h. Cell lysates were probed with indicated antibodies. DAPK inactivation is expressed in %, whereas TNF-treated cells alone are considered as a control (set as 100%). Changed levels of p-LIMK^{Thr508} and p-cofilin^{Ser3} are shown in %, compared to TNF-treated cells with normal DAPK activity as a control (set as 100%). (B) HCT116 cells were transiently transfected with indicated concentration of DAPK-specific or scrambled siRNA oligonucleotides for 24 h prior to TNF-treatment. Cell lysates were prepared at 24 and 48 h following TNF-stimulation and subjected to immunoblot analysis with antibodies as indicated. (C) HCT116 cells were 24 h transfected with DAPK construct or empty vector and 24 h TNF-treated. Cell lysates were immunoblotted with antibodies as indicated (l.exp = longer exposure; sh.exp = shorter exposure). Untreated HCT116 cells (c) served as a control. The band intensities were quantified by densitometry analysis in three independent experiments; the control was adjusted to one.

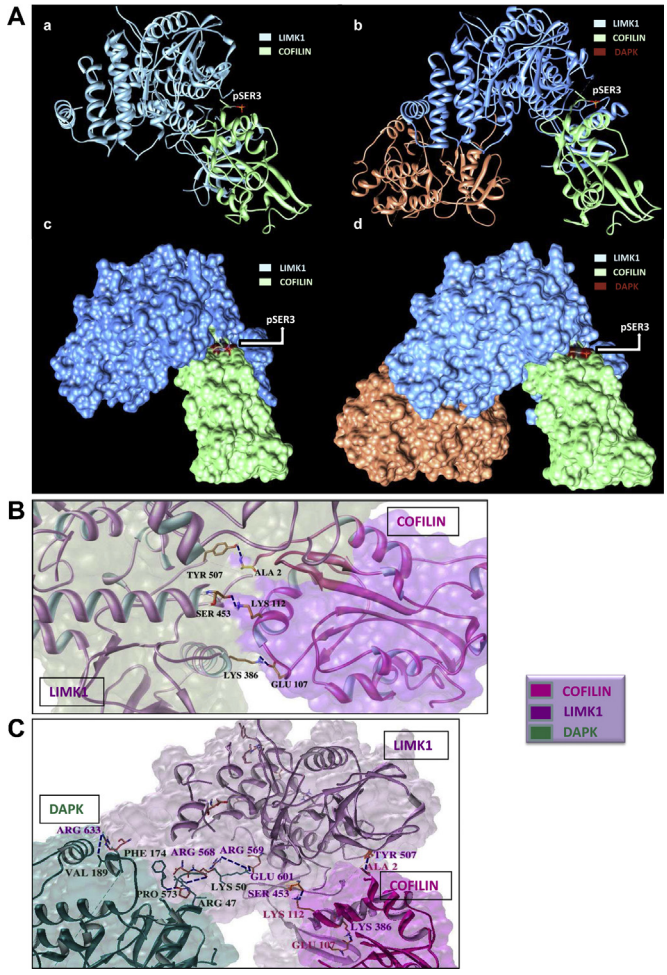

Fig. 4. Interaction of DAPK with LIMK/cofilin is stabilizing the complex. (A) Pictures (a and c) present docked complexes of cofilin (PDB ID: 1Q8G) – LIMK1 (PDB ID: 3S95). Pictures (b and d) show docked complexes of cofilin–LIMK and DAPK (PDB ID: 1JKS). (B) Picture of putative interactions between the cofilin and LIMK in the docked complex of cofilin (PDB ID: 1Q8G)–LIMK (PDB ID: 3S95). (C) Picture of putative interactions between the cofilin, LIMK and DAPK in the docked complex of cofilin (PDB ID: 1Q8G)–LIMK (PDB ID: 3S95) and DAPK (PDB ID: 1JKS).

bond (HBPLUS and PIC server) revealed 3 hydrogen bonds between the cofilin and the kinase domain of LIMK as shown Table 1a. In the docked DAPK/LIMK/cofilin complex, a new interaction is observed between lysine112 of cofilin and asparagine455 of LIMK (Table 1a and b). In total, the bonding pattern showed interactions between 8 residues of LIMK and DAPK (Table 1b and Fig. 4C). These results suggested that there is no direct interaction between cofilin and DAPK (Fig. 4A, b and d, 4B and C). Threonine508 of LIMK was not found within the 5 Å zone around p-cofilin^{Ser3} in the LIMK/cofilin complex. When the DAPK/LIMK/cofilin complex was formed by docking, the residue threonine508 of LIMK moved closer into the 5 Å zone of interaction (Table 2) suggesting a further stabilization of the LIMK/cofilin complex. In the next step, we used cluster scores of the complexes from the ClusPro server to analyze the energy profiles of the docked LIMK/cofilin and docked DAPK/LIMK/cofilin complexes. As expected, the energy of the DAPK/LIMK/cofilin complex was found to be less than that of the LIMK/cofilin complex by 24.5% (the percentage of energy difference between the score of both the structures) (Fig. 4A, a and b). Accordingly, the energy scores of the clusters of the two complexes also differ by 26.1% (Fig. 4A, c and d). This modeling supports our findings of a DAPK/LIMK/cofilin complex and suggests that DAPK may serve a structural role in its assembly.

An in vitro pulldown experiment with the recombinantly expressed, purified proteins (GST/His DAPK, LIMK and cofilin) to confirm the existence of such a tripartite protein complex was not successful. There are several reasons such as the lack of commercially available full lengths constructs of DAPK and LIMK, their possible too transient interaction or the lack of other yet unknown assembly factors.

Alternatively, we have performed confocal immunofluorescence analyses of cells stained for LIMK, DAPK and cofilin (Fig. 5) to verify this complex. In the absence of TNF stimulation, LIMK, DAPK and cofilin are homogeneously distributed in the cytoplasm. However, upon TNF-treatment we observed a striking redistribution of all three proteins to the perinuclear compartment (Fig. 5). We can therefore not rule out that e.g., subcellular membrane compartments are required for the assembly of the proposed DAPK/LIMK/cofilin complex which have to be identified and investigated in future in more detail.

3.3. DAPK/LIMK/p-cofilin^{Ser3} complex participates in TNF-induced apoptosis

Next we asked the question if the newly identified interaction partners of DAPK contribute to TNF-induced apoptosis. In the first step, LIMK-overexpression was performed in HCT116 cells with or without TNF-treatment. The level of active caspase3, a key marker of apoptosis, was 1.9-fold higher in TNF-treated LIMK overexpressing cells than in vector control-transfected HCT116 cells (Fig. S2B). In line with this observation, LIMK si RNA resulted in a decrease in caspase3 cleavage 24 h after TNF-treatment compared to cells treated with the scrambled siRNA subjected to TNF-treatment (Fig. S2A), but was not completely attenuated. Thus caspase3-independent mechanisms cannot be excluded. Nevertheless, these data suggest that LIMK is participating in TNF-induced apoptosis.

We next assessed whether the change in the phosphorylation status of p-cofilin^{Ser3} affects TNF-induced apoptotic signaling. HCT116 cells were transfected with cofilin wt and phospho-mimicking mutants cofilin^{Glu3} and cofilin^{Asp3} of the inactivation site cofilin^{Ser3} (Nishimura et al., 2006), and exposed to TNF. As shown in Fig. S3A, cells expressing cofilin regardless of its phosphorylation status showed similar fold increases (between 2- and 3-fold changes) of active caspase3 in transfected cells upon TNF-stimulation compared to transfected untreated HCT116 cells (Fig. S3A). These data were confirmed by Annexin V-staining (Fig. S3B), supporting a model in which LIMK modulates the activity of caspase3, whereas p-cofilin^{Ser3} is also correlated with apoptosis but is not a trigger of the pro-apoptotic signaling cascade.

To further test this hypothesis, we studied the distribution and intensity of p-cofilin^{Ser3} by immunofluorescence (IF) (Fig. S4). Our results revealed that IF intensity of p-cofilin^{Ser3} was significantly increased in TNF-treated apoptotic cells with condensed chromatin (Fig. S4A–C). Moreover, the relationship between p-cofilin^{Ser3} IF intensity and DNA-Hoechst staining intensity was approximately linear, with a correlation coefficient of $r = 0.67$ (Fig. S4B). IF detection of apoptosis using co-staining of Annexin V with p-cofilin^{Ser3} demonstrated that p-cofilin^{Ser3} was significantly accumulated in Annexin V positive cells after TNF-treatment in comparison to untreated control cells (Fig. 6A and C). In agreement with these findings, we observed increased membrane bleb formation in cells with high p-cofilin^{Ser3} accumulation by phase-contrast imaging (Fig. 6B). These observations led us to evaluate p-cofilin^{Ser3} accumulation in apoptotic, detached and adherent HCT116 cells. Detached cells showed a clear loss in paxillin levels, which is associated with diminished cell adhesion (Figs. 7 and 8). Although the DAPK/LIMK/cofilin complex seems to be dissociated there is still signaling in the detached cells showing after TNF treatment a progressive increase in the levels of p-cofilin^{Ser3}, caspase 8, 9 and 3 cleavage compared to the adherent cell population. This increase was ~12-fold for p-cofilin^{Ser3}, ~15-fold for active caspase3, ~15-fold for caspase8 and ~13-fold for caspase9 (Figs. 7 and 8). This confirmed that phosphorylation of cofilin on serine3 is an associated event in TNF-induced apoptosis in HCT116 cells and strengthens our hypothesis drawn from p-cofilin^{Ser3} mutants. DAPK that is suggested to be the scaffold protein for the complex is lost in the detached cells. Interestingly, also pLIMK^{Thr508} cannot be found in the supernatant, suggesting that activated LIMK in detached cells seems to be no longer needed for the permanent activation of cofilin during apoptosis (Figs. 7 and 8). To better understand why there is this increase of p-cofilin^{Ser3} level without DAPK and p-LIMK^{Thr508}, we have checked for the expression of chronophin, a cofilin phosphatase (Gohla et al., 2005). Interestingly protein expression of chronophin was down-regulated in the supernatants possibly leading to stabilization of p-cofilin^{Ser3} levels in detached apoptotic cells (Fig. 7). A graphical model summarizing the

Table 2
Residues present in a zone of 5 Å from Serine3 of cofilin.

Docked complex of cofilin–LIMK LIMK1	Docked complex of cofilin–LIMK–DAPK
Cofilin residues Alanine 2, Glycine 4, Valine 5, Aspartate 122, Alanine 123, Lysine 126, Serine 119	**Cofilin residues** Alanine 2, Glycine 4, Valine 5, Aspartate 122, Alanine 123, Lysine 126, Serine 119
LIMK residues Val 486, Met 485, Tyr 507	**LIMK residues** Val 486, Met 485, Tyr 507, Thr 508

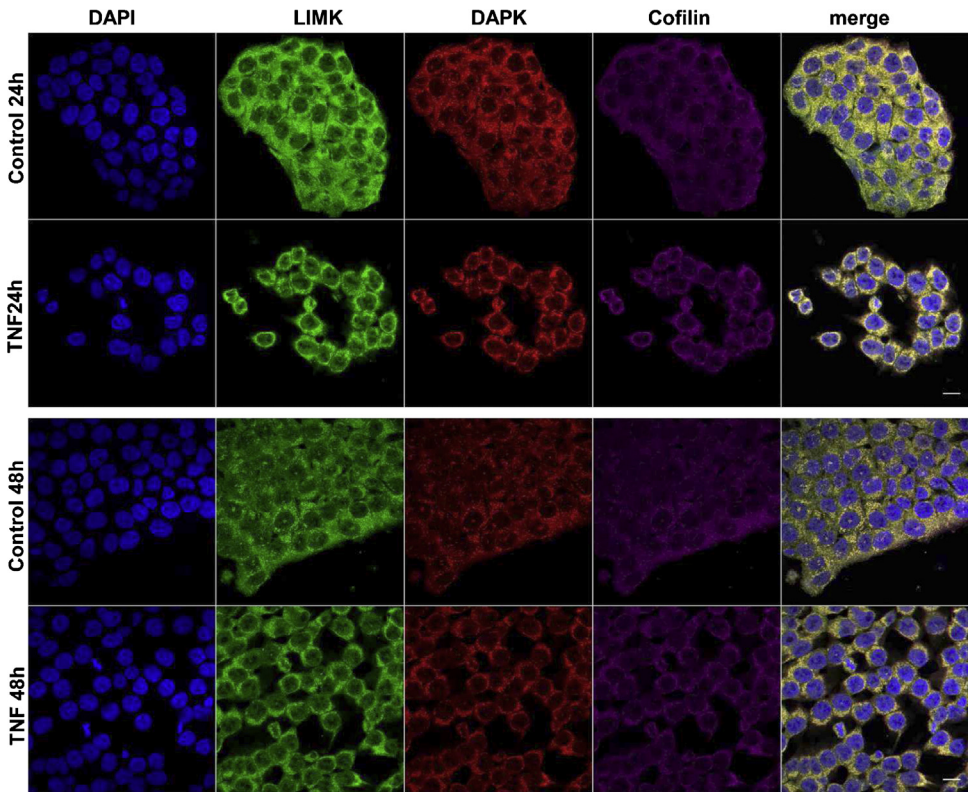

Fig. 5. Distribution and co-localization of LIMK, DAPK and cofilin after the TNF-treatment. Confocal immunofluorescence image of endogenous LIMK (green), DAPK (red), cofilin (magenta) and DAPI (blue) staining in fixed HCT116 cells treated with TNF (0.66 ng/ml). The same confocal microscopy setup was used for all representative images. Excitation was only seen with the appropriate laser. Bar 10 μm.

expression of different participating proteins under TNF-treatment in apoptotic detached and adherent HCT116 cells is given in Fig. 8.

4. Discussion

The serine/threonine kinase DAPK plays an important role in a wide range of different cell death modes (Lin et al., 2010). To date, only a limited number of proteins that interact with DAPK have been identified. Recently, we have described a novel interaction between the MAPkinase p38 and DAPK in TNF-induced apoptosis of colorectal cancer cells (Bajbouj et al., 2009). To better understand how DAPK mediates caspase3-dependent apoptotic cell death, we performed a peptide array screen to identify phosphorylated targets under TNF treatment. The peptide array showed pronounced cofilin phosphorylation at serine3. In the Western blot analysis we confirmed a phosphorylation of its up-stream kinase LIMK at threonine508 in response to TNF. Although there was a consistent LIMK activation and subsequent cofilin inactivation pattern after TNF treatment, the broad variation in the time frame between 24 and 48 h cannot be fully explained. Because LIMK was shown to be involved in cell cycle progression (Manetti, 2012), we might speculate that this variation results from cells in different phases of the cell cycle. Due to high cytotoxicity of the combination of lipofectamin with starvation this experimental proof was technically impossible. In a set of experiments that are discussed below, we then identified DAPK as an interaction partner of LIMK. Our data suggest that DAPK serves as a scaffold of the LIMK/cofilin complex.

It has been shown that DAPK induces cell death through an increase in DAPK catalytic activity and subsequent phosphorylation of target proteins (Shang et al., 2005; Yamamoto et al., 2002), but its multidomain structure enables also a close physical interaction with other proteins (Bialik and Kimchi, 2006). To obtain a mechanistic insight into the role of DAPK in LIMK/cofilin signaling, we studied the effect of DAPK inhibition, siRNA knockdown and overexpression on the phosphorylation status of LIMK and cofilin under TNF treatment. After DAPK inhibition with potent and selective DAPK inhibitor (Gandesiri et al., 2012; Okamoto et al., 2010), the LIMK/p-cofilin^{Ser3} signaling was diminished. Furthermore, the levels of p-cofilin^{Ser3} and p-LIMK^{Thr508} correlated with the DAPK expression status as shown by DAPK siRNA experiments. DAPK-overexpression led to increased p-cofilin^{Ser3} levels, surprisingly however without any detectable change in p-LIMK^{Thr508} levels. Because the cofilin^{Ser3}-residue is not located within a consensus DAPK motif, we speculate that DAPK-overexpression might (directly or indirectly) block the activity of cofilin phosphatases. Another explanation could be a possible interplay between cofilin serine3 residue and another phosphorylation site. Inspection of the human cofilin sequence revealed the presence of a DAPK–phosphorylation consensus motif (Lin et al., 2010) around serine24 (**R**ks**S**^{24}), but after mutating serine24 to Ala/Glu, we could not detect any influence on cofilin^{Ser3} phosphorylation and TNF-induced apoptosis (unpublished data). Moreover, DAPK-phosphorylation consensus motifs (Lin et al., 2010) are present in Cdc42 (Kuo et al., 2006), and can also be detected in the amino acid sequences of ROCK1, Rho A, and PAK1 (LIMK up-stream kinases). Although these proteins were not identified in our peptide array, we cannot exclude their involvement in our model. There also exist DAPK motifs in the LIMK protein sequence, but the 8 interaction residues proposed in the 3D model do not include any phosphorylatable amino acid. Another potential connection between DAPK and cofilin may be provided by 14-3-3 proteins, which are known to bind to DAPK (Henshall et al., 2003) and to stabilize phosphorylated cofilin (Gohla and Bokoch, 2002). Interestingly, the 3D structural model suggests no direct interaction between DAPK and cofilin. The

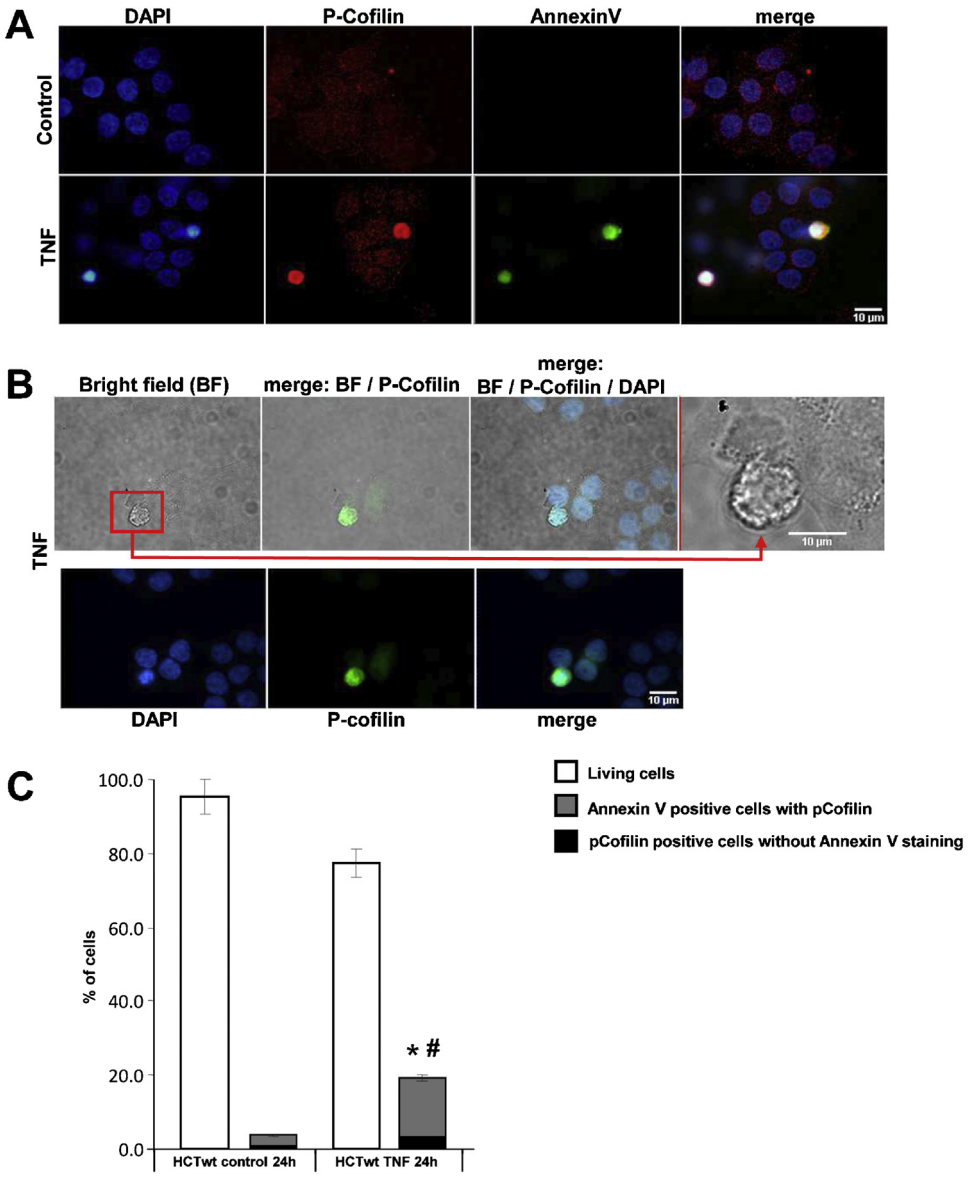

Fig. 6. Accumulation of p-cofilin^{Ser3} in TNF-induced apoptotic cells. (A) TNF-induced apoptosis detected by immunofluorescence using Annexin V (green), DAPI (blue) and p-cofilin^{Ser3} (red) staining in HCT116 cells. Bar, 10 μm. (B) Phase-contrast imaging was performed to detect bleb formation of HCT116 cells treated with TNF and stained with p-cofilin^{Ser3} antibody and DAPI. Bar, 10 μm. (C) Quantification of fixed HCT116 cells stained with p-cofilin^{Ser3} antibody and Annexin V with and without TNF-treatment. Annexin V staining was performed to detect apoptotic cells. 100–150 cells were scored. Error bars represent the SEM based on two independent experiments. ($^{*}p \leq 0.05$ as compared with control cells Annexin V positive with pCofilin; $^{\#}p \leq 0.05$ as compared with control cells pCofilin positive).

evidence of cofilin in the DAPK immunoprecipitation instead suggests a strong LIMK/cofilin interaction. The energy analysis on the complexes of LIMK/cofilin and of DAPK/LIMK/cofilin could explain that DAPK provides further stability to the complex. Thus, we propose that both the kinase activity and scaffolding functions of DAPK are important in TNF-induced apoptosis.

The significance of cofilin activation/inactivation during apoptosis is only poorly understood. To date, there are only few reports showing a role of cofilin in inducing cell death under oxidative stress (Campos et al., 2009; Hsieh et al., 2010; Klamt et al., 2009; Rehklau et al., 2012). Studying the dephosphorylated, active form of cofilin1, Chua et al., 2003, reported its mitochondrial translocation preceding the release of cytochrome c, indicating a role in the initiation phase of apoptosis. Other studies described a participation of active cofilin in growth-stimulating processes (Samstag et al., 1991, 1994, 1996; Saito et al., 1994).

Interestingly, treatment of endothelial cells with a cytokine cocktail containing IL-1, IL-6 and TNF increased the phosphorylation of cofilin together with the formation of actin stress fibers (Campos et al., 2009). Similarly, inhibition of p-cofilin^{Ser3} dephosphorylation by the serine phosphatase inhibitor okadaic acid was accompanied by apoptosis (Samstag et al., 1996). By varying the cofilin phosphorylation using p-cofilin^{Ser3} mutants, we demonstrated that the expression of the pseudophosphorylated (cofilin^{Glu3} and cofilin^{Asp3}) and nonphosphorylatable mutant cofilin^{Ala3} did not significantly alter TNF-induced apoptosis in comparison with cofilin wt expression. Thus, we suggest that p-cofilin^{Ser3} is an indicator of TNF-induced apoptosis and does not further trigger the apoptotic signal. In this regard, p-cofilin^{Ser3} levels were found to be increased in TNF-induced apoptotic cells with condensed chromatin, pronounced membrane blebs and Annexin V up-regulation. In detached cells, we see a massive accumulation

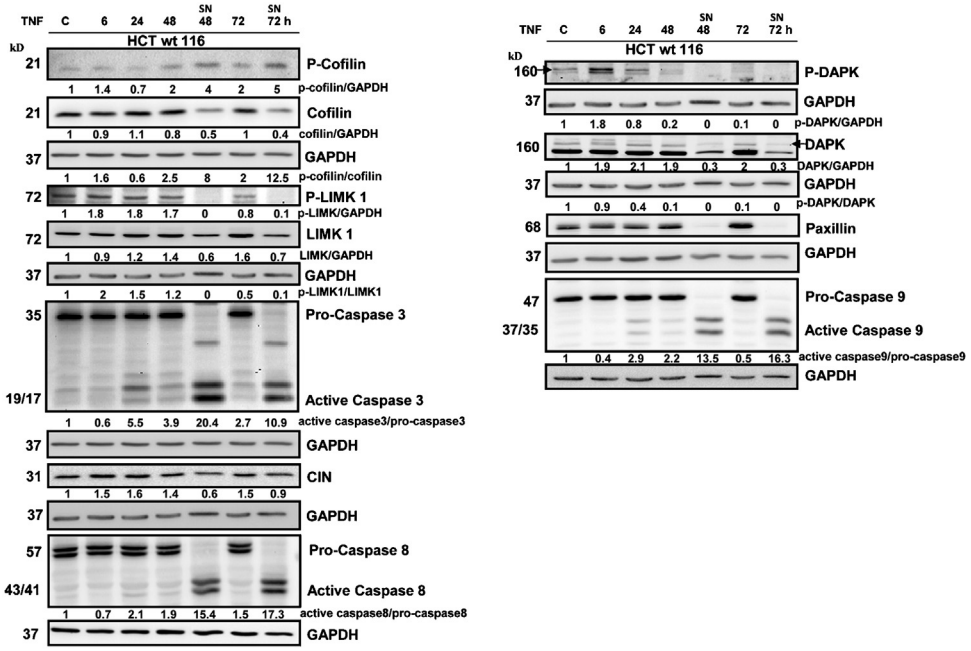

Fig. 7. Accumulation of p-cofilin^{Ser3} in apoptotic, non-adherent and adherent HCT116 cells. Lysates of adherent HCT116 subjected to TNF (0.66 ng/ml), and non-adherent, dead HCT116 cells collected from the supernatants (SN) 48 and 72 h after TNF treatment, were analyzed by Western blotting with antibodies as indicated. The band intensities were quantified by densitometry analysis; the control was adjusted to one. The data are representative of three independent experiments.

of inactive p-cofilin^{Ser3} which has lost the actin filament disrupting activity. According to Wiggan et al. (2012), cofilin silencing could induce a crucial disturbance of normal homeostatic actin-myosin cytoarchitecture, resulting in bleb formation. The high levels of activated caspases might mediate the cleavage of further cytoskeletal proteins such as myosin light chain, actin, vimentin, and paxillin (Byun et al., 2001; Mashima et al., 1999; Moretti et al., 2002; Shim et al., 2001). The reinforced caspase 8, 9, and 3 activation could be explained as a cell death induced by loss of cell adhesion (anoikis) as described for ceramide-induced cell death (Widau et al., 2010). Although there is a role of DAPK in anoikis this form of cell death might be not associated with the described DAPK/LIMK/cofilin complex under TNF stimulus. The loss of pLIMK^{Thr508} and DAPK in detached cells suggests that the multiprotein complex consisting of pLIMK^{Thr508}, cofilin, and DAPK is abrogated in detached apoptotic cells and its signaling is interrupted. Obviously TNF-treated cells have committed to caspase-dependent apoptosis prior to detachment from the culture plate. Here upon TNF a striking redistribution of LIMK, DAPK, and cofilin to the perinuclear compartment was observed. Whereas assembly of these three proteins was not associated with condensation of the chromatin, adherent apoptotic cells were positively marked by p-cofilin^{Ser3} and p-LIMK^{Thr508} co-localization. In summary, we present a novel pro-apoptotic multi-protein complex including DAPK, LIMK and cofilin that is reinforced following TNF-treatment. 3D structural modeling suggests that DAPK can act as a scaffold to integrate the LIMK1/cofilin1 complex. Furthermore, we suggest that p-cofilin^{Ser3} is a marker but not a trigger of TNF-induced apoptosis in HCT116 cells, and is mainly responsible for the cytoskeletal changes that apoptotic cells undergo.

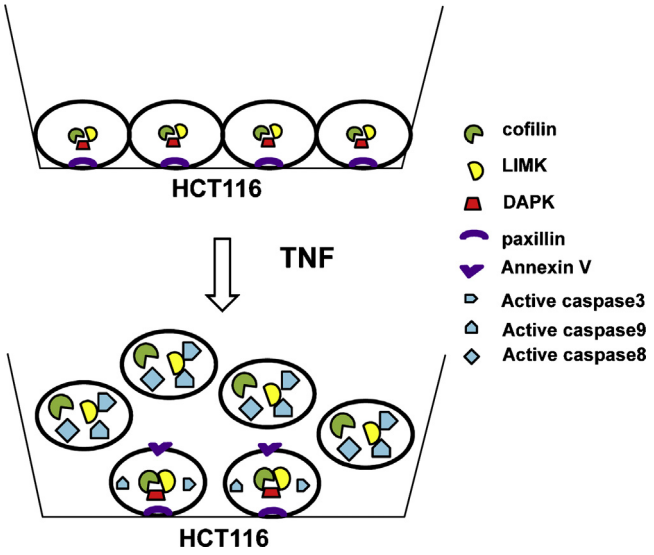

Fig. 8. A graphical model summarizing the expression of different participating proteins under TNF-treatment in apoptotic detached and adherent HCT116 cells. The multiprotein complex is formed in control cells and it was reinforced under TNF in adherent cells. DAPK is lost from the complex in detached cells as scaffold protein for the LIMK/cofilin complex.

Funding

This work was supported by a research grant of the Deutsche Forschungsgemeinschaft (SCHN477-9-2 to R.S.S), the Manfred-Stolte-Stiftung (to R.S.S.) and by a research grant from the German Cancer Aid (Deutsche Krebshilfe, No. 106696/TP 5 to T.F.).

Appendix A. Supplementary data

Supplementary data associated with this article can be found, in the online version, at http://dx.doi.org/10.1016/j.biocel.2013.05.013.

References

Aizawa H, Wakatsuki S, Ishii A, Moriyama K, Sasaki Y, Ohashi K, et al. Phosphorylation of cofilin by LIM-kinase is necessary for semaphorin 3A-induced growth cone collapse. Nature Neuroscience 2001;4:367–73.

Arber S, Barbayannis FA, Hanser H, Schneider C, Stanyon CA, Bernard O, et al. Regulation of actin dynamics through phosphorylation of cofilin by LIM-kinase. Nature 1998;393:805–9.

Bajbouj K, Poehlmann A, Kuester D, Drewes T, Haase K, Hartig R, et al. Identification of phosphorylated p38 as a novel DAPK-interacting partner during TNFα-induced apoptosis in colorectal tumour cells. American Journal of Pathology 2009;175:557–70.

Bamburg JR, McGough A, Ono S. Putting a new twist on actin. ADF/cofilins modulate actin dynamics. Trends in Cell Biology 1999;9:364–70.

Beltrami A, Chaikuad A, Daga N, Elkins JM, Mahajan P, Savitsky P, et al. Crystal structure of the human LIMK1 kinase domain in complex with staurosporine; 2013 [in press].

Benderska N, Chakilam S, Hugle M, Ivanovska J, Gandesiri M, Schulze-Lührmann J, et al. Apoptosis signalling activated by TNF in the lower gastrointestinal tract-review. Current Pharmaceutical Biotechnology 2012;13:2248–58.

Bernstein BW, Bamburg JR. ADF/cofilin: a functional node in cell biology. Trends in Cell Biology 2010;4:187–95.

Bialik S, Kimchi A. DAP-kinase as a target for drug design in cancer and diseases associated with accelerated cell death. Seminars in Cancer Biology 2004;14:283–94.

Bialik S, Kimchi A. The death-associated protein kinases: structure, function, and beyond. Annual Review of Biochemistry 2006;75:189–210.

Byun Y, Chen F, Chang R, Trivedi M, Green KJ, Cryns VL. Caspase cleavage of vimentin disrupts intermediate filaments and promotes apoptosis. Cell Death and Differentiation 2001;8:443–50.

Campos SB, Ashworth SL, Wean S, Hosford M, Sandoval RM, Hallett MA, et al. Cytokine-induced F-actin reorganization in endothelial cells involves RhoA activation. American Journal of Physiology – Renal Physiology 2009;296:487–95.

Chua BT, Volbracht C, Tan KO, Li R, Yu VC, Li P. Mitochondrial translocation of cofilin is an early step in apoptosis induction. Nature Cell Biology 2003;5:1083–9.

Cohen O, Feinstein E, Kimchi A. DAP-kinase is a Ca^{2+}/calmodulin-dependent, cytoskeletal-associated protein kinase, with cell death-inducing functions that depend on its catalytic activity. EMBO Journal 1997;16:998–1008.

Deiss LP, Feinstein E, Berissi H, Cohen O, Kimchi A. Identification of a novel serine/threonine kinase and a novel 15-kD protein as potential mediators of the gamma interferon-induced cell death. Genes and Development 1995;9:15–30.

Gandesiri M, Chakilam S, Ivanovska J, Benderska N, Ocker M, Di Fazio P, et al. DAPK plays an important role in panobinostat-induced autophagy and commits cells to apoptosis under autophagy deficient conditions. Apoptosis 2012 [Epub ahead of print].

Gohla A, Birkenfeld J, Bokoch GM. Chronophin, a novel HAD-type serine protein phosphatase, regulates cofilin-dependent actin dynamics. Nature Cell Biology 2005;7:21–9.

Gohla A, Bokoch GM. 14-3-3 regulates actin dynamics by stabilizing phosphorylated cofilin. Current Biology 2002;12:1704–10.

Henshall DC, Araki T, Schindler CK, Shinoda S, Lan JQ, Simon RP. Expression of death-associated protein kinase and recruitment to the tumor necrosis factor signaling pathway following brief seizures. Journal of Neurochemistry 2003;86:1260–70.

Hsieh YC, Rao YK, Wu CC, Huang CY, Geethangili M, Hsu SL, et al. Methyl antcinate A from *Antrodia camphorata* induces apoptosis in human liver cancer cells through oxidant-mediated cofilin- and Bax-triggered mitochondrial pathway. Chemical Research in Toxicology 2010;23:1256–67.

Inbal B, Cohen O, Polak-Charcon S, Kopolovic J, Vadai E, Eisenbach L, et al. DAP kinase links the control of apoptosis to metastasis. Nature 1997;390:180–4.

Inbal B, Shani G, Cohen O, Kissil JL, Kimchi A. Death-associated protein kinase-related protein 1, a novel serine/threonine kinase involved in apoptosis. Molecular and Cellular Biology 2000;20:1044–54.

Klamt F, Zdanov S, Levine RL, Pariser A, Zhang Y, Zhang B, et al. Oxidant-induced apoptosis is mediated by oxidation of the actin-regulatory protein cofilin. Nature Cell Biology 2009;11:1241–6.

Kobayashi M, Nishita M, Mishima T, Ohashi K. MAPKAPK-2-mediated LIM-kinase activation is critical for VEGF-induced actin remodeling and cell migration. EMBO Journal 2006;25:713–26.

Kögel D, Reimertz C, Düssmann H, Mech P, Scheidtmann KH, Prehn JH. The death associated protein (DAP) kinase homologue Dlk/ZIP kinase induces p19ARF- and p53-independent apoptosis. European Journal of Cancer 2003;39:249–56.

Kozakov D, Hall DR, Beglov D, Brenke R, Comeau SR, Shen Y, et al. Achieving reliability and high accuracy in automated protein docking: Cluspro, PIPER, SDU, and stability analysis in CAPRI rounds 13–19. Proteins 2010;78:3124–30.

Kuo JC, Lin JR, Staddon JM, Hosoya H, Chen RH. Uncoordinated regulation of stress fibers and focal adhesions by DAP-kinase. Journal of Cell Science 2003;116:4777–90.

Kuo JC, Wang WJ, Yao CC, Chen RH. The tumor suppressor DAPK inhibits cell motility by blocking the integrin-mediated polarity pathway. Journal of Cell Biology 2006;172:619–31.

Lin Y, Hupp TR, Stevens C. Death-associated protein kinase (DAPK) and signal transduction: additional roles beyond cell death. FEBS Journal 2010;277:48–57.

Manetti F. LIM kinases are attractive targets with many macromolecular partners and only a few small molecule regulators. Medicinal Research Reviews 2012;32:968–98.

Mashima T, Naito M, Tsuruo T. Caspase-mediated cleavage of cytoskeletal actin plays a positive role in the process of morphological apoptosis. Oncogene 1999;18:2423–30.

Mathew SJ, Haubert D, Krönke M, Leptin M. Looking beyond death: a morphogenetic role for the TNF signalling pathway. Journal of Cell Science 2009;122:1939–46.

Moon A, Drubin DG. The ADF/cofilin proteins: stimulus–responsive modulators of actin dynamics. Molecular Biology of the Cell 1995;6:1423–31.

Moretti A, Weig HJ, Ott T, Seyfarth M, Holthoff HP, Grewe D, et al. Essential myosin light chain as a target for caspase-3 in failing myocardium. Proceedings of the National Academy of Sciences of the United States of America 2002;99:11860–5.

Mouneimne G, Desmarais V, Sidani M, Scemes E, Wang W, Song X, et al. Spatial and temporal control of cofilin activity is required for directional sensing during chemotaxis. Current Biology 2006;16:2193–205.

Nishimura Y, Yoshioka K, Bernard O, Bereczky B, Itoh K. A role of LIM kinase 1/cofilin pathway in regulating endocytic trafficking of EGF receptor in human breast cancer cells. Histochemistry and Cell Biology 2006;126:627–38.

Nishita M, Tomizawa C, Yamamoto M, Horita Y, Ohashi K, Mizuno K. Spatial and temporal regulation of cofilin activity by LIM kinase and Slingshot is critical for directional cell migration. Journal of Cell Biology 2005;171:349–59.

Niwa R, Nagata-Ohashi K, Takeichi M, Mizuno K, Uemura T. Control of actin reorganization by Slingshot, a family of phosphatases that dephosphorylate ADF/cofilin. Cell 2002;108:233–46.

Okamoto M, Takayama K, Shimizu T, Muroya A, Furuya T. Structure-activity relationship of novel DAPK inhibitors identified by structure-based virtual screening. Bioorganic and Medicinal Chemistry 2010;18:2728–34.

Petsko GA, Ringe D. Bonds that stabilize folded proteins in Protein Structure and Function. New Science Press; 2004. p. 10–1.

Pollard TD, Borisy GG. Cellular motility driven by assembly and disassembly of actin filaments. Cell 2003;112:453–65.

Pope BJ, Zierler-Gould KM, Kuhne R, Weeds AG, Ball LJ. Solution structure of human cofilin: actin binding, pH sensitivity, and relationship to actin-depolymerizing factor. Journal of Biological Chemistry 2004;279:4840–8.

Raveh T, Kimchi A. DAPkinase-a proapoptotic gene that functions as a tumor suppressor. Experimental Cell Research 2001;264:185–92.

Rehklau K, Gurniak CB, Conrad M, Friauf E, Ott M, Rust MB. ADF/cofilin proteins translocate to mitochondria during apoptosis but are not generally required for cell death signaling. Cell Death and Differentiation 2012;19:958–67.

Saito T, Lamy F, Roger PP, Lecocq R, Dumont JE. Characterization and identification as cofilin and destrin of two thyrotropin- and phorbol ester-regulated phosphoproteins in thyroid cells. Experimental Cell Research 1994;212:49–61.

Samstag Y, Bader A, Meuer SC. A serine phosphatase is involved in CD2-mediated activation of human T lymphocytes and natural killer cells. Journal of Immunology 1991;147:788–94.

Samstag Y, Dreizler EM, Ambach A, Sczakiel G, Meuer SC. Inhibition of constitutive serine phosphatase activity in T lymphoma cells results in phosphorylation of pp19/cofilin and induces apoptosis. Journal of Immunology 1996;156:4167–73.

Samstag Y, Eckerskorn C, Wesselborg S, Henning S, Wallich R, Meuer SC. Costimulatory signals for human T-cell activation induce nuclear translocation of pp19/cofilin. Proceedings of the National Academy of Sciences of the United States of America 1994;91:4494–8.

Scanlon M, Laster SM, Wood JG, Gooding LR. Cytolysis by tumor necrosis factor is preceded by a rapid and specific dissolution of microfilaments. Proceedings of the National Academy of Sciences of the United States of America 1989;86:182.

Shang T, Joseph J, Hillard CJ, Kalyanaraman B. Death-associated protein kinase as a sensor of mitochondrial membrane potential: role of lysosome in mitochondrial toxin-induced cell death. Journal of Biological Chemistry 2005;280:34644–53.

Shim SR, Kook S, Kim JI, Song WK. Degradation of focal adhesion proteins paxillin and p130cas by caspases or calpains in apoptotic rat-1 and L929 cells. Biochemical and Biophysical Research Communications 2001;286:601–8.

Tereshko V, Teplova M, Brunzelle J, Watterson DM, Egli M. Crystal structures of the catalytic domain of human protein kinase associated with apoptosis and tumor suppression. Natural Structural Biology 2001;8:899–907.

Wang WJ, Kuo JC, Yao CC, Chen RH. DAP-kinase induces apoptosis by suppressing integrin activity and disrupting matrix survival signals. Journal of Cell Biology 2002;159:169–79.

Widau RC, Jin Y, Dixon SA, Wadzinski BE, Gallagher PJ. Protein phosphatase 2A (PP2A) holoenzymes regulate death-associated protein kinase (DAPK) in ceramide-induced anoikis. Journal of Biological Chemistry 2010;285:13827–38.

Wiggan O, Shaw AE, DeLuca JG, Bamburg JR. ADF/cofilin regulates actomyosin assembly through competitive inhibition of myosin II binding to F-actin. Developmental Cell 2012;22:530–43.

Yamamoto M, Hioki T, Ishii T, Nakajima-Iijima S, Uchino S. DAP kinase activity is critical for C(2)-ceramide-induced apoptosis in PC12 cells. European Journal of Biochemistry 2002;269:139–47.

Yang N, Higuchi O, Ohashi K, Nagata K, Wada A, Kangawa K, et al. Cofilin phosphorylation by LIM-kinase 1 and its role in Rac-mediated actin reorganization. Nature 1998;393:809–12.

Yoshioka K, Foletta V, Bernard O, Itoh K. A role for LIM kinase in cancer invasion. Proceedings of the National Academy of Sciences of the United States of America 2003;100:7247–52.